BIOCHEMISTRY
including biophysical chemistry & molecular biology
Article

Biochemistry **2011,** *50,* 1359–1367 1359
DOI: 10.1021/bi101749s

The Cullin-RING E3 Ubiquitin Ligase CRL4−DCAF1 Complex Dimerizes via a Short Helical Region in DCAF1†

Jinwoo Ahn,*,‡,§ Zach Novince,‡,§ Jason Concel,‡,§ Chang-Hyeock Byeon,‡,§ Alexander M. Makhov,§ In-Ja L. Byeon,‡,§ Peijun Zhang,‡,§ and Angela M. Gronenborn*,‡,§

‡*University of Pittsburgh Center for HIV Protein Interactions and* §*Department of Structural Biology, University of Pittsburgh School of Medicine, Pittsburgh, Pennsylvania 15260, United States*

Received November 1, 2010; Revised Manuscript Received January 7, 2011

ABSTRACT: The cullin4A-RING E3 ubiquitin ligase (CRL4) is a multisubunit protein complex, comprising cullin4A (CUL4), RING H2 finger protein (RBX1), and DNA damage-binding protein 1 (DDB1). Proteins that recruit specific targets to CRL4 for ubiquitination (ubiquitylation) bind the DDB1 adaptor protein via WD40 domains. Such CRL4 substrate recognition modules are DDB1- and CUL4-associated factors (DCAFs). Here we show that, for DCAF1, oligomerization of the protein and the CRL4 complex occurs via a short helical region (residues 845−873) N-terminal to DACF1's own WD40 domain. This sequence was previously designated as a LIS1 homology (LisH) motif. The oligomerization helix contains a stretch of four Leu residues, which appear to be essential for α-helical structure and oligomerization. *In vitro* reconstituted CRL4−DCAF1 complexes ($CRL4^{DCAF1}$) form symmetric dimers as visualized by electron microscopy (EM), and dimeric $CRL4^{DCAF1}$ is a better E3 ligase for *in vitro* ubiquitination of the UNG2 substrate compared to a monomeric complex.

Protein degradation is a highly regulated process carried out by the ubiquitin−proteasome system (*1*−*3*). It involves covalent modification of protein substrates with multiple copies of ubiquitin (Ub)[1] chains, followed by proteolysis of the Ub-tagged proteins by the 26S proteasome (*4*, *5*). Posttranslational ubiquitination is extremely diverse, variable in multimer length and linkage type. While attachment of a single Ub module affects protein localization (*6*), polyubiquitination at different Lys residues of Ub targets proteins for degradation or regulation of activity (*7*−*9*). Ub modification involves a concerted series of enzymatic reactions. The first enzyme, E1, activates Ub in an Mg-ATP-dependent manner, creating a covalent thiolester-linked E1∼Ub complex (Ub(T)) with a second Ub bound at the adenylation active site (Ub(A)). Subsequently, the thiolester-linked Ub(T) is transferred to a reactive Cys on a cognate E2 conjugating enzyme by transesterification, and Ub-loaded E2s are released from E1s for substrate attachment by E3s (*10*−*12*). Two different classes of E3 ligases have been characterized that either contain a HECT (homologous to E6-AP C-terminus) or a RING (really interesting new gene) domain. The RING domain protein RBX1 forms modular complexes with several homologous cullin scaffold subunits (CUL1 to CUL7; reviewed in ref *13*). Each CUL-RBX1 heterodimer uses a specific adaptor protein to form a multisubunit complex, referred to as a cullin-RING ubiquitin ligase (CRL1−7). The RING domain mainly functions as a docking site for the E2 enzyme (*14*−*16*) at the C-terminus of the cullin, while the adaptor proteins bind to the N-terminus of the cullin and position substrate receptors and target proteins for ubiquitination (*13*, *17*, *18*). One of the adaptor proteins is DDB1 (DNA damage-binding protein 1), a 127 kDa modular protein that contains three seven-bladed β-propeller WD40 domains (*19*−*21*). DDB1 specifically associates with CUL4 and binds more than 50 different DCAFs (DDB1- and CUL4-associated factors) that function as substrate receptor proteins (*22*−*25*). DCAF proteins also contain a WD40 domain that is used for interacting with DDB1(*21*, *24*−*26*).

For most DCAF proteins, neither cellular function nor targets have been identified. Those cellular targets that have been identified were shown to function in chromatin remodeling, DNA replication, cell cycle regulation, and apoptosis (*27*, *28*). Intriguingly, Vpr, one of the four accessory proteins encoded by HIV-1, interacts with DCAF1, possibly targeting unidentified cellular factors for degradation and mediating Vpr's biological activity in G2/M-phase cell-cycle arrest (*29*−*37*).

It has been argued that in CRL−substrate receptor complexes differences in substrate sizes may present a problem for polyubiquitination given the variable distance between the catalytic site on E2 and the target Lys residue(s) on the substrate. If present, structural constraints imposed by the rigid cullin scaffold in CRLs can be resolved by positioning a flexible hinge somewhere in the complex. This appears to be the achieved by NEDD8 modification at the C-terminus of CUL, shown to impart conformational flexibility onto CUL and RBX1, thereby facilitating polyubiquitination of the substrates (*38*, *39*). An

†This work was supported by the National Institutes of General Medical Sciences (NIH Grant P50GM082251 to A.M.G. and GM08-5043 to P.Z.).

*To whom correspondence should be addressed. J.A.: tel, 412-383-6933; fax, 412-648-9008; e-mail, jia12@pitt.edu. A.M.G.: tel, 412-648-9959; fax, 412-648-9008; e-mail, amg100@pitt.edu.

[1]Abbreviations: Ub, ubiquitin; E1, ubiquitin-activating enzyme; E2, ubiquitin-conjugating enzyme; E3, ubiquitin ligase; ATP, adenosine triphosphate; RING, really interesting new gene; CUL, cullin; CRL, cullin-RING ubiquitin ligase; DDB1, DNA damage-binding protein 1; DCAF1, DDB1-CUL4A-associated factor 1; HIV-1, human immunodeficiency virus 1; Vpr, viral protein, regulatory; LIS1, lissencephaly associated gene 1; LisH, LIS 1 homology; CRL4, DDB1-cullin4A-RING ubiquitin ligase; $CRL4^{DCAF1}$, CRL4 in complex with DCAF1; EM, electron microscopy; SEC-MALS, size-exclusion column chromatography coupled to in-line multiangle light scattering.

Published on Web 01/12/2011

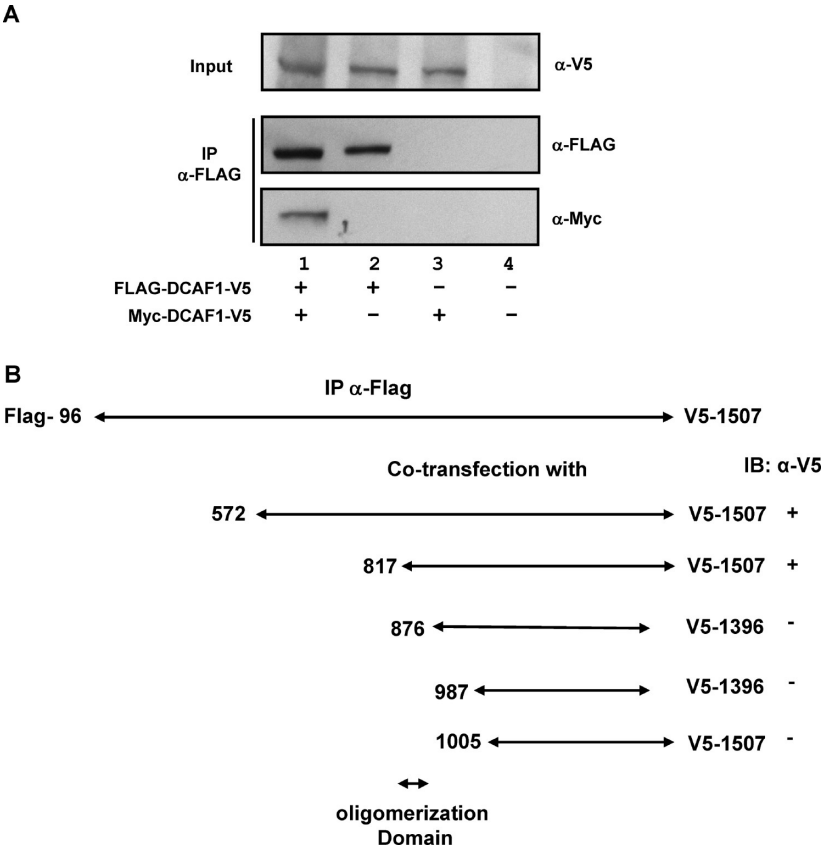

FIGURE 1: DCAF1 oligomerizes via a putative LisH motif *in vivo*. (A) N-Terminally FLAG-tagged and C-terminally V5-tagged DCAF1 (FLAG-DCAF1-V5, residues 96−1507) was transiently coexpressed with N-terminally Myc-tagged and C-terminally V5-tagged DCAF1 (Myc-DCAF1-V5, residues 96−1507) in SF9 insect cells. Cell lysates were immunoprecipitated with anti-FLAG agarose affinity gel, and pull-down mixtures were analyzed by immunoblotting with anti-FLAG and anti-Myc antibodies (IP), after separation by SDS−PAGE and transfer to nitrocellulose. 5% of total cell lysates were also immunoblotted with anti-V5 antibody (input). (B) FLAG-DCAF1-V5 was transiently coexpressed in SF9 cells with several deletion constructs of DCAF1 (residues 572−1507, 817−1507, 876−1396, 987−1396, and 1005−1507) containing the V5 tag at their C-termini. Each cell lysate was subjected to immunoprecipitation with anti-FLAG agarose affinity gel, and pull-down mixtures were analyzed by immunoblotting with anti-V5 antibody. Constructs pulled down by FLAG-DCAF1-V5 are labeled by (+) and those not pulled down by (−).

alternative mechanism could exploit dimerization, and indeed, for several CRLs, dimerization via the substrate receptor proteins has been reported (reviewed in ref *18*). Dimerization allows for polyubiquitination *in trans* as well as *in cis* without affecting the substrate affinity (*40*−*44*).

Here, we report that DCAF1 can oligomerize through an α-helical region that was originally identified as a LisH motif. This region is located N-terminal to the WD40 domain, although quite distant with ca. 200 residues separating the two regions. *In vitro* biochemical studies and electron microscopy of $CRL4^{DCAF1}$ complexes reveal that the E3 ubiquitin ligase indeed forms an oligomeric supramolecular complex that could aid to accommodate a variety of substrate sizes for ubiquitination.

EXPERIMENTAL PROCEDURES

Cloning and Construction of Plasmids. The cDNA for DCAF1 was purchased from Open Biosystems and codes for residues 97−1507. DCAF1 constructs comprising amino acids 572−1507, 817−1507, 876−1396, 987−1396, and 1005−1507 were cloned into the pIZ/V5-His vectors (Invitrogen), resulting in His_6 and V5 tags at the C-termini of the protein constructs. In addition, N-terminally FLAG-tagged or Myc-tagged DCAF1 constructs, encoding residues 96−1507, were cloned into pIZ/V5-His vectors, respectively. Site-directed mutagenesis was carried out on pIZ/V5-His DCAF1 817−1507 using QuickChange kits (Stratagene) to create the L850E/L851E and L852E/L853 mutants. Constructs coding for residues 809−876 were amplified from the pIZ/V5-His DCAF1 817−1507 WT DNA and the two mutants and cloned into pET32 vectors (Invitrogen). Other DCAF1 constructs coding for residues 809−902 and 841−883 were also cloned into the pET32 vectors. The pET32 vectors were modified to contain a TEV protease recognition site between the thioredoxin fusion partner and the target protein (*45*). For baculoviruses expressing DCAF1 proteins, constructs coding for 817−1507, 987−1396, and 1005−1507 were cloned into the pENT vector (Invitrogen). Recombinant baculoviruses expressing C-terminally His_6-tagged DCAF1 proteins were prepared using Baculodirect C-term (Invitrogen) and pENT-DCAF1 vectors, according to the manufacturer's protocol. Nucleotide sequences were verified for the entire coding regions of all constructs.

Expression and Purification of Proteins. Thioredoxin (pET32)-tagged DCAF1 809−876 WT, L850E/L851E, L852E/L853E mutant, DCAF1 809−902, and 841−883 constructs containing His_6 tag between thioredoxin and the TEV protease recognition site were expressed in *Escherichia coli* Rosetta 2 (DE3), cultured in Luria−Bertani media, using 0.4 mM IPTG for induction and growth at 18 °C for 16 h. The DCAF1 809−876 WT, L850E/L851E, L852E/L853E mutant constructs contain an additional C-terminal His_6 tag. Uniform $^{13}C/^{15}N$ labeling of DCAF1 809−876 WT, DCAF1 809−902, and DCAF1 841−883 proteins was carried out by growth in modified medium using $^{15}NH_4Cl$ and/or [$^{13}C_6$]glucose as sole nitrogen and carbon sources,

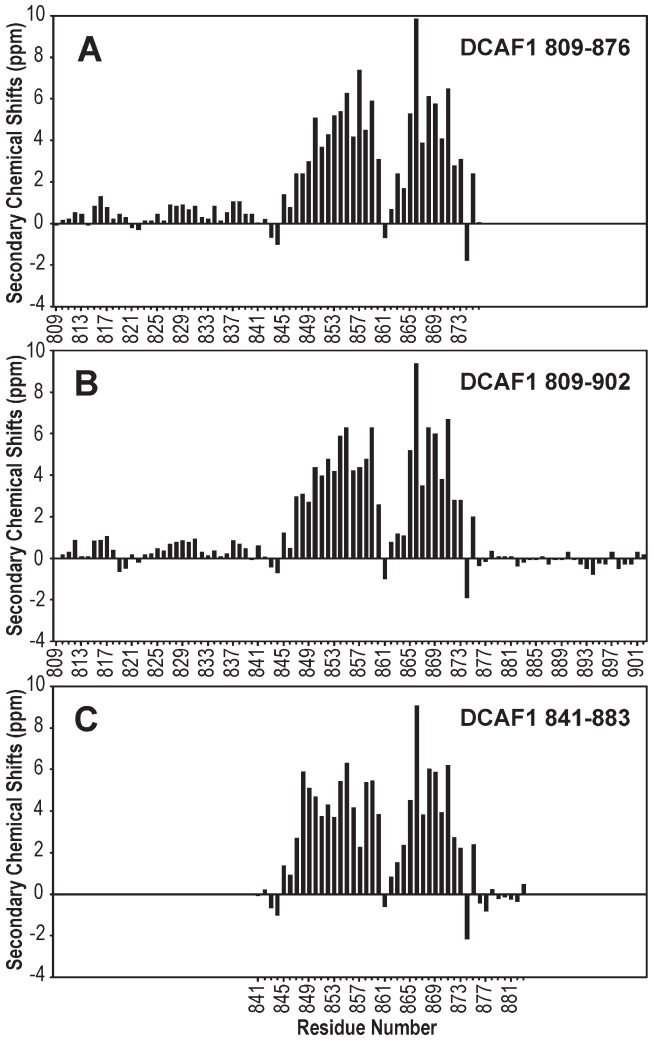

FIGURE 2: Secondary structure characterization of isolated DCAF1 peptides by NMR. (A−C) Secondary chemical shifts, ΔC_α minus ΔC_β (*48*), for DCAF1 809−876 (A), 809−902 (B), and 841−883 (C) are shown along the amino acid sequence. ΔC_α and ΔC_β values were calculated for all assigned resonances by subtracting measured C_α and C_β shifts from random coil values (*47*).

respectively. Soluble forms of His_6-tagged proteins were purified using 5 mL Ni-NTA columns (GE Heatlthcare), and aggregated materials were removed by gel-filtration column chromatography using a Hi-Load Superdex200 16/60 column (GE Healthcare), equilibrated with a buffer containing 25 mM sodium phosphate, pH 7.5, 150 mM NaCl, 1 mM DTT, 10% glycerol, and 0.02% sodium azide. Thioredoxin-tagged DCAF1 proteins were digested with TEV protease, and DCAF1 proteins were purified over an 8 mL MONO Q column (GE Healthcare), equilibrated with 25 mM Tris-HCl, pH 8.5, and 0.02% azide, using a 0−1 M NaCl gradient for elution. C-Terminally His_6-tagged DCAF1 817−1507, 1005−1507, and 987−1396 proteins were coexpressed with N-terminally His_{10}- and FLAG-tagged DDB1 in SF21 insect cells (Invitrogen). The N-terminally His_6-tagged RBX1 and CUL4A were also coexpressed in SF21 cells. Expression of proteins in insect cells and purification were performed as described previously (*46*). For preparation of multiprotein complexes composed of CUL4A, RBX1, DDB1, and DCAF1 proteins, all components were mixed at equimolar ratios, and the protein complexes were purified over an 8 mL MONO Q column (GE Healthcare) at pH 7.5, using a 0−1 M NaCl gradient for elution. Purified complexes were analyzed by SDS−PAGE and native PAGE and visualized by Coomassie Blue staining. All other proteins used in this report were prepared as previously described (*46*).

Insect Cell Cultures and Transient Transfection. SF9 cells (Invitrogen) were cultured in SF-900 II SFM medium containing 2% fetal bovine serum. Cells were plated in 10 cm plates at 90% confluency 2 h prior to transient transfection. The cells were cotransfected with a total of 16 μg of pIZ/V5-His plasmids coding for the various DCAF1 constructs as indicated using Cellfectin II (Invitrogen), according to the manufacturer's protocol. Cells were harvested 48 h after transfection and subjected to immunoprecipitation as described below.

Immunoprecipitation and Immunoblotting. Transiently transfected SF9 cells were harvested and treated with 400 μL of a lysis buffer containing phosphate-buffered saline (PBS), 5% glycerol, 1% Tween 20, 1% NP-40, 0.2 mM phenylmethanesulfonyl fluoride, and protease inhibitor cocktail (EMD Biosciences). The lysates were incubated with 40 μL of anti-FLAG agarose affinity gel for 4 h, and the beads were washed four times with 500 μL of the lysis buffer. Immunoprecipitates were eluted from the beads with 50 μL of sample loading buffer or FLAG peptides at a concentration of 100 μg/mL. Eluted proteins were separated by SDS−PAGE and probed by immunoblotting. For detection of proteins, anti-Myc (Sigma), anti-FLAG (Sigma), and anti-V5 (Sigma) antibodies were used.

NMR Spectroscopy. All NMR experiments were recorded at 25 °C using a Bruker AVANCE600 spectrometer, equipped with a 5 mm triple-resonance, *z*-axis gradient cryoprobe, on samples containing 0.3 mM $^{13}C/^{15}N$-labeled DCAF1 809−876, 809−902, and 841−883 peptides in 25 mM sodium phosphate buffer, pH 6.5, 150 mM sodium chloride, and 0.02% sodium azide. Backbone and C_β resonance assignments of DCAF1 809−876, 809−902, and 841−883 were carried out using 2D $^1H-^{15}N$ HSQC and 3D HNCACB and HN(CO)CACB experiments. Secondary structure elements of these peptides were obtained based on secondary chemical shifts using ΔC_α minus ΔC_β with ΔC_α and ΔC_β values calculated by subtracting random coil C_α and C_β shifts from the measured values (*47*, *48*).

Multiangle Light Scattering. The molecular masses of protein complexes were obtained using an analytical Superdex200 column (1 cm × 30 cm; GE Healthcare) with in-line multiangle light scattering (HELEOS, Wyatt Technology), variable wavelength UV (Agilent 1100 Series; Agilent Technology), and refractive index (Optilab rEX; Wyatt Technology) detection. Typically, about 100 μL of 2 mg/mL protein solutions was injected into the column that was preequilibrated with a buffer containing 25 mM sodium phosphate, pH 7.5, 150 mM NaCl, 5% glycerol, and 0.02% sodium azide at a flow rate of 0.5 mL/min at room temperature. Light scattering data were analyzed using the ASTRA program (Wyatt Technology).

Circular Dichroism (CD) Spectroscopy. Far-UV (195−250 nm) CD spectra of DCAF1 809−876 WT, L850E/L851E, and L852E/L853E mutants were recorded at a concentration of 3.3 μM in 2.5 mM sodium phosphate buffer, pH 7.5, and 15 mM NaCl at 25 °C using a JASCO-810 (Easton, MD) spectrophotometer. Data were collected with 0.5 nm intervals and averaged 10 times.

Electron Microscopy (EM) Analysis. The purified $CRL4^{DCAF1}$ complex composed of RBX1-CUL4A-DDB1-DCAF1 817−1507 at a concentration of 0.8 mg/mL was diluted 50-fold and deposited onto glow-discharged carbon foil grids, blotted with filter paper, and stained with 2% uranyl acetate. The

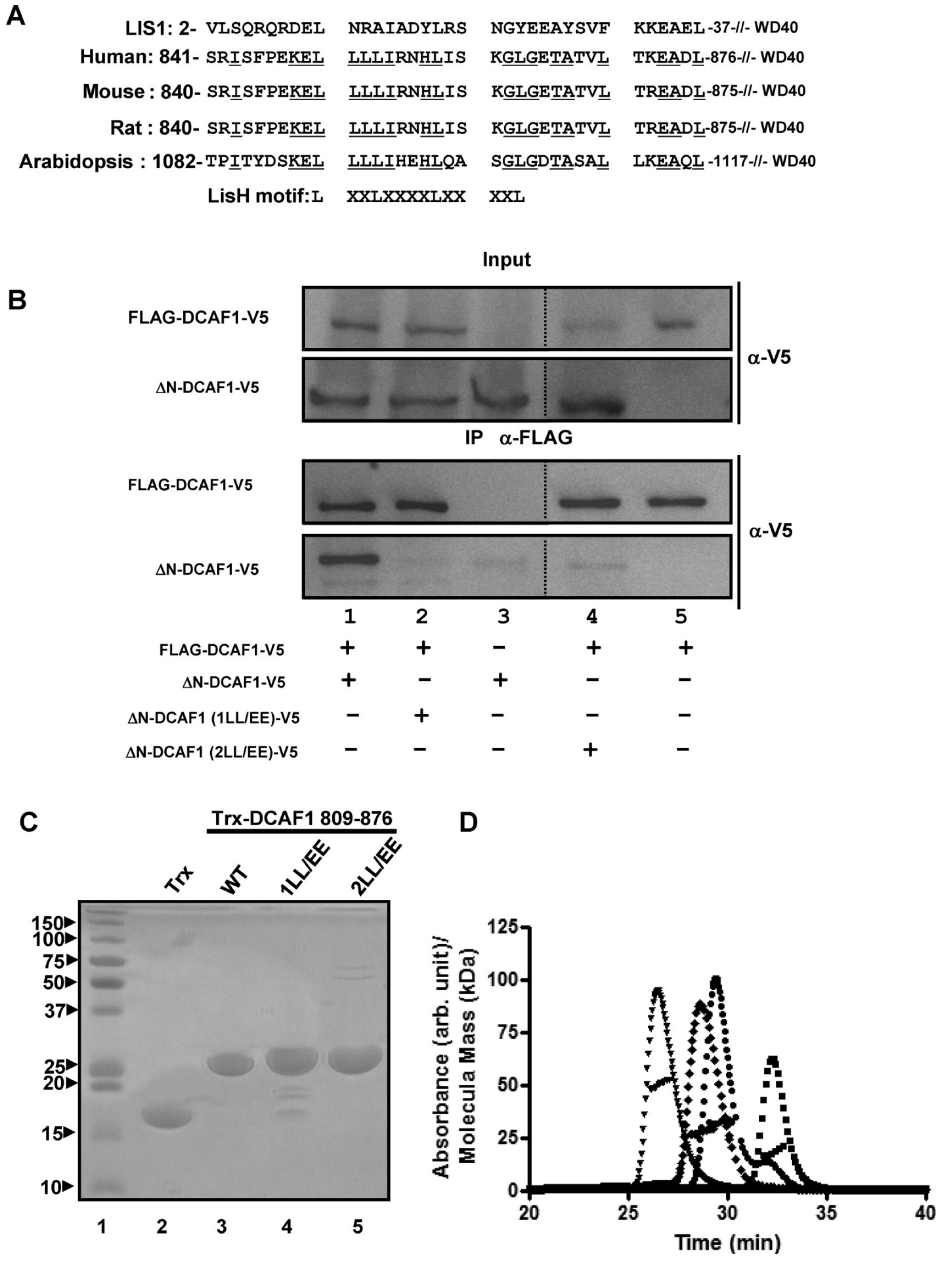

FIGURE 3: The four Leu region is critical for oligomerization of DCAF1. (A) Sequence alignment of putative LisH domains in orthologous DCAF1s. Identical amino acid residues are underlined, and the LisH motif, L-X_2-L-X_{3-5}-L-X_{3-5}-L, is displayed at the bottom. X represents any amino acid. (B) FLAG-DCAF1-V5 (encoding residues 96−1507) was transiently coexpressed with the N-terminally deleted DCAF1 (ΔN-DCAF1-V5, residues 817−1507), site-directed mutants ΔN-DCAF1 (1LL/EE)-V5, and ΔN-DCAF1 (2LL/EE)-V5, respectively in SF9 insect cells. 1LL/EE corresponds to the Leu850Glu, Leu851Glu double mutant and 2LL/EE to the Leu852Glu, Leu853Glu double mutant. Cell lysates were immunoprecipitated with anti-FLAG agarose affinity gel. Proteins bound to antibodies were separated by SDS−PAGE and subjected to immunoblotting with anti-V5 antibody after transfer to nitrocellulose. (C) The DCAF1 region corresponding to residues 809−876 and the 1LL/EE and 2LL/EE mutants thereof were expressed and purified from *E. coli* as thioredoxin (Trx) fusion proteins. Trx and the three Trx-DCAF1 proteins were separated by SDS−PAGE and stained with Coomassie Brilliant Blue. (D) Multiangle light scattering of purified Trx-DCAF1 fusion proteins and Trx as a control. Each protein (ca. 2 mg/mL) was injected into an analytical Superdex200 gel filtration column at a flow rate of 0.5 mL/min. The UV (A_{280}) elution profiles of Trx-DCAF1 809−876 WT (▼), Trx-DCAF1 809−876 1LL/EE (●), Trx-DCAF1 809−876 2LL/EE (◆), and Trx (■) are shown. The estimated molecular masses from the scattering data are shown across the elution peaks.

grids were examined at 200 kV with a TF20 electron microscope (FEI, Hillsboro, OR). Images were recorded with a 4K × 4K Gatan CCD camera (Gatan, Inc., Warrendale, PA) at a nominal magnification of 50000× and underfocus values ranging from 1.5 to 3.0 μm.

Image Processing of EM. EM images were processed using the EMAN image analysis software (*49*). Individual particles were boxed manually with 208 × 208 pixels (2.14 Å/pixel), normalized, and combined to yield one raw image stack file. A total of 1900 individual particle images was selected, band-pass-filtered, and aligned with respect to their center of mass. The aligned raw projection images were classified using reference-free multivariance statistical analysis and averaged within each class.

In Vitro Ubiquitination Assays. Typically, E1 (UBA1, 0.2 μM), E2 (UbcH5b, 2.5 μM), and the E3 ligase (0.2 or 0.4 μM DDB1-CUL4A-RBX1 complexed with the various DCAF1 constructs as indicated) were incubated at 37 °C with 0.5 μM NusA-Vpr-ΔC (residues 1−79), 1 μM UNG2, and 2.5 μM

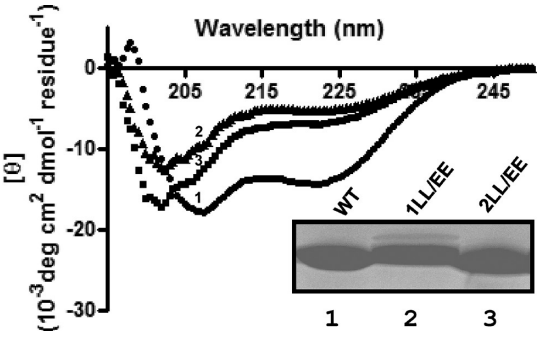

FIGURE 4: Secondary structure characterization of WT and mutant LisH motif peptides by CD. Circular dichroism (CD) spectra of WT DCAF1 809−876 (1, ●), 1LL/EE 809−876 (2, ▲), and 2LL/EE 809−876 (3, ■) recorded at 3.3 μM in a buffer containing 2.5 mM sodium phosphate, pH 7.5, and 15 mM NaCl, at 25 °C. Data were collected at 0.5 nm intervals, scanned from 250 to 195 nm, and averaged over 10 measurements. The inset shows the SDS−PAGE analysis of the peptides used for CD.

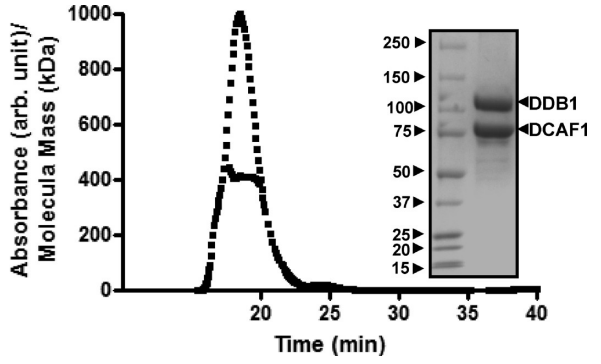

FIGURE 5: Characterization of the DDB1−DCAF1 complex by SEC-MALS and SDS−PAGE. The DDB1−DCAF1 817−1507 protein complex was injected into an analytical gel filtration column at a flow rate of 0.5 mL/min. The UV (A_{280}) elution profile and the estimated molecular mass from the scattering data are shown across the elution peaks. The protein complex was separated by SDS−PAGE, and proteins were visualized by Coomassie Brilliant Blue.

His_6-FLAG-tagged ubiquitin in a buffer containing 10 mM Tris-HCl, pH 7.5, 150 mM NaCl, 5% glycerol, 20 units/mL pyrophosphatase, 2 mM DTT, and 5 mM ATP for various lengths of time. Reactions were stopped by heating the samples in SDS−Laemmli buffer at 95 °C for 5 min. The extent of ubiquitination was determined by immunoblotting with anti-FLAG or anti-UNG2 (Abnova) antibodies, after separation of the reaction mixtures on 4−20% gradient SDS−PAGE, and transfer to nitrocellulose.

RESULTS AND DISCUSSION

DCAF1 Proteins Oligomerize When Ectopically Expressed in Insect Cells. It is known that several CRLs dimerize via substrate receptor proteins (*18*, *40*−*42*, *50*). In addition, the DCAF1 sequence contains a Lissencephaly type 1-like homology motif (LisH) (*51*) between residues 846 and 876, known to mediate dimerization. It therefore seemed prudent to evaluate whether oligomerization of DCAF1 may occur, especially since during protein expression and purification of a long DCAF1 construct (residues 96−1507) aggregation was observed, with DDB1-DCAF1 complexes eluting in the void volume of a Superdex200 gel-filtration column (Ahn et al., unpublished results). The apparent discrepancy between the expected molecular mass (280 kD) of the complex and the experimental behavior warranted further examination.

In order to assess whether oligomerization of DCAF1 occurred, coimmunoprecipitation of transiently expressed, differentially tagged DCAF1 proteins in insect cells was carried out. Specifically, both N-terminally Myc-tagged DCAF1 and N-terminally FLAG-tagged DCAF1 (residue 96−1507) were transiently coexpressed in SF9 cells, with both constructs containing a V5 tag at their C-termini. Cell lysates were subjected to immunoprecipitation with anti-FLAG antibodies, and indeed, interaction between the Myc-tagged and FLAG-tagged DCAF1 proteins was observed (Figure 1A, lane 1).

The oligomerization domain was mapped by coexpressing various truncated DCAF1 constructs (residues 572−1507, 817−1507, 876−1396, 987−1396, and 1005−1507), tagged with the V5 epitope at their C-termini together with the FLAG-tagged DCAF1 (residues 96−1507). Immunoprecipitation with anti-FLAG antibodies and subsequent immunoblotting with anti-V5 antibodies of coexpressed DCAF constructs revealed that the putative LisH motif, comprising residues 846−876, needed to be present for stable interaction (Figure 1B). In particular, the 876−1396, 987−1396, or 1005−1507 constructs failed to coimmunoprecipitate with the FLAG-tagged DCAF1 96−1507 bait, while 572−1507 or 817−1407 constructs did. These data provided strong evidence for a possible direct interaction between DCAF1 proteins, mediated by residues 817−876 that contain the putative LisH motif. However, association of DCAF1 proteins via other endogenous cellular proteins could not be ruled out. To directly confirm the homooligomerization of DCAF1 proteins, the isolated peptide region implicated in the association was investigated as described below.

Secondary Structure of a DCAF1-LisH Peptide in Solution. The secondary structure of the LisH motif containing region of DCAF1 was investigated by NMR. Three different lengths of peptides were prepared, DCAF1 809−876, DCAF1 809−902, and DCAF1 841−883 (Figure 2). Qualitative structural characterization of the DCAF1 809−876 WT peptide analyzing secondary chemical shifts ($\Delta\delta C_\alpha - \Delta\delta C_\beta$) clearly suggested that the C-terminal half of the peptide (Phe845−Glu873) exhibited an α-helical conformation, indicated by a stretch of large positive values of secondary chemical shifts for Glu847−Ser860 and Leu862−Glu873, with a break at Lys861 (Figure 2A). Most of the residues in the N-terminal half of DCAF1 809−876 also exhibit positive secondary chemical shifts, albeit too small to suggest that a helical structure is present. In order to unambiguously delineate the helix boundaries, the peptide was extended at its C-terminus up to residue 902 (Figure 2B). The secondary chemical shifts for this longer peptide revealed that the helix terminates at Glu873. Further, a shorter DCAF1 peptide (residues 841−883) also displays similar boundaries for the helical region (Figure 2C). These data confirm that the putative LisH motif (residues 846−876) is embedded in an α-helical structure, in agreement with the well-characterized helical LisH motif of LIS1 (*52*, *53*). One notable different feature of the region surrounding the LisH motif in DCAF1 is that the residues following the motif display random coil properties. The canonical LisH motif is often followed by an extended coiled-coil segment with a short helical segment connecting these two regions (*52*, *53*). However, these coiled-coil segments do not contribute to dimerization and exhibit random coil properties as isolated fragments (*53*).

The Region of the Four Leu Repeat Is Essential for α*-Helical Structure and Oligomerization of DCAF1*. The LisH motif is present in numerous eukaryotic proteins, frequently N-terminal to WD40 domains (*51*), and in DCAF1 the prototypical

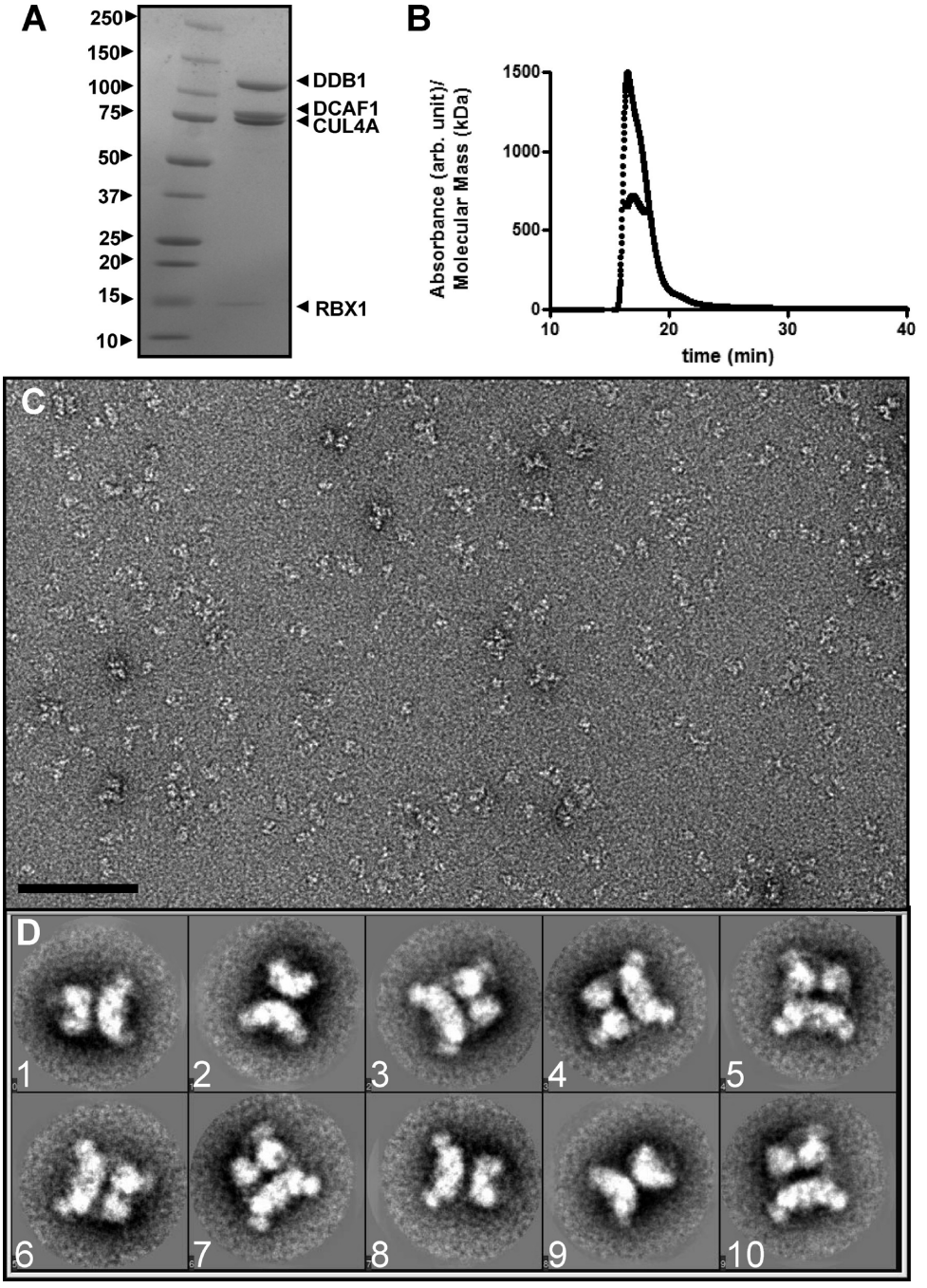

FIGURE 6: Electron microscopy of $CRL4^{DCAF1}$ E3 ligase complexes. (A) SDS−PAGE analysis of the $CRL4^{DCAF1}$ E3 ligase complex, assembled with CUL4A, RBX1, DDB1, and DCAF1 (residues 817−1507). Each component of the complex is indicated. (B) SEC-MALS analysis of the $CRL4^{DCAF1}$ E3 ligase complex. The protein complex was injected into an analytical gel filtration column at a flow rate of 0.5 mL/min, and the data were analyzed as described in Experimental Procedures. The estimated molecular mass is shown across the elution peak. (C) Electron micrograph of negatively stained $CRL4^{DCAF1}$ complexes (scale bar, 100 nm). (D) Selected 2D class averages of $CRL4^{DCAF1}$ complex particles selected from the micrograph. Some class averages show near mirror symmetry suggesting the presence of a 2-fold axis in the complexes.

L-X_2-L-X_{3-5}-L-X_{3-5}-L sequence (*51*) is located at positions 850−863. Sequence alignment of the pertinent DCAF1 region with orthologous sequences and human LIS1 is provided in Figure 3A. Interestingly, the LisH motif of DCAF1 contains four Leu residues adjacent to Ile854, the residue that corresponds to the critical Ile15 residue in the dimer interface of the LIS1 structure (*52*, *54*). In order to assess whether these Leu residues are important for oligomer formation, we constructed two mutants of DCAF1, ΔN-L850E/L851E DCAF1-V5 (residues 817−1507 of L850E/L851E DCAF1 with a C-terminal V5 tag; 1LL/EE) and ΔN-L852E/L853E DCAF1-V5 (residues 817−1507 of L852E/L853E DCAF1 with a C-terminal V5 tag; 2LL/EE). Coexpression of either mutant with N-terminally FLAG-tagged and C-terminally V5-tagged DCAF1 (FLAG-DCAF1-V5, residues 96−1507) did not result in efficient coimmunoprecipitation (Figure 3B, lanes 2 and 4). In contrast, WT ΔN-DCAF1-V5 coprecipitated efficiently with FLAG-DCAF1-V5 (Figure 3B, lane 1). These data suggest that residues within the Leu850−Leu853 stretch are essential for the interaction between different DCAF1 molecules.

To directly confirm that the four Leu repeat in the LisH motif of DCAF1 is responsible for oligomerization, both

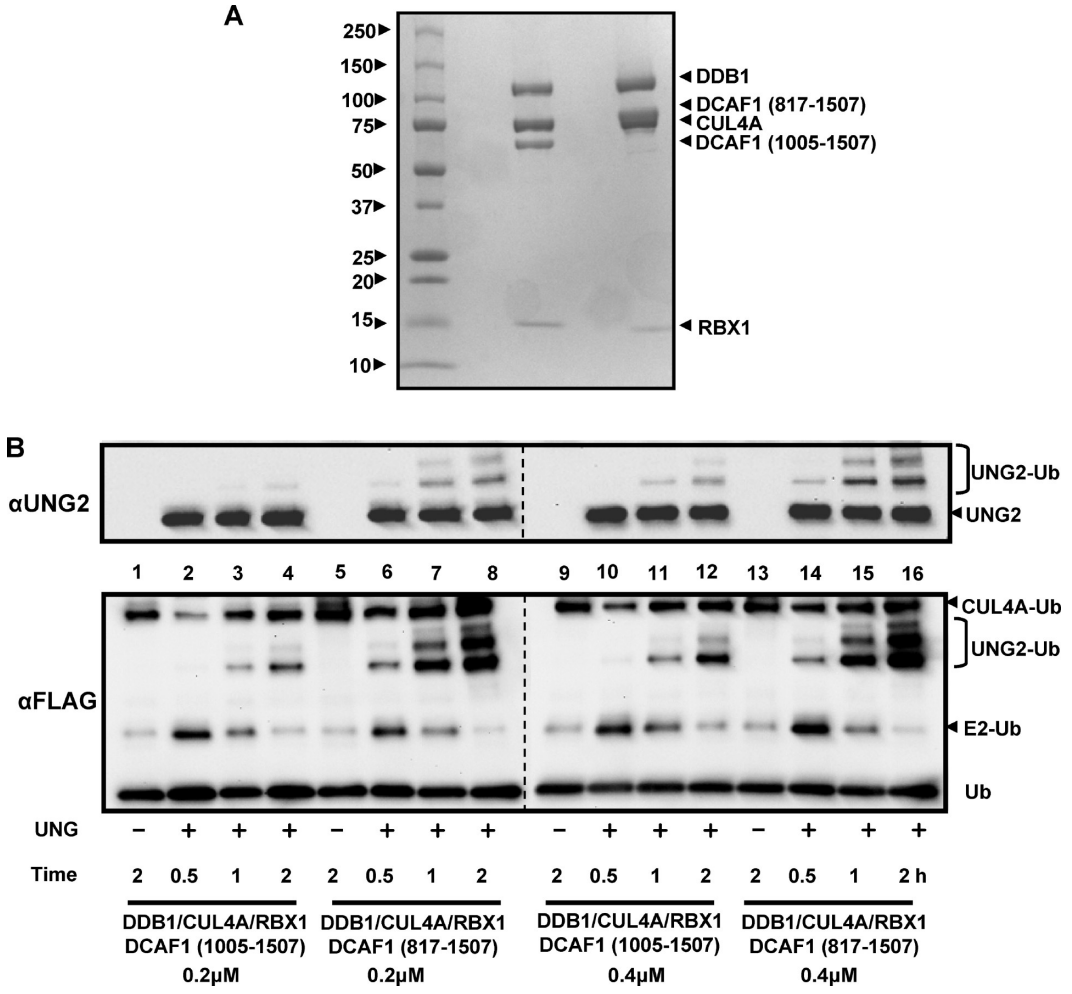

FIGURE 7: Ubiquitination activity of monomeric and dimeric $CRL4^{DCAF1}$. (A) 20 pmol of monomeric CRL4 complex bound to DCAF1 (1005−1507) and dimeric CRL4 bound to DCAF1 (817−1507) separated by SDS−PAGE and visualized with Coomassie Blue. (B) Time course of UNG2 ubiquitination with dimeric $CRL4^{DCAF1}$ and monomeric $CRL4^{DCAF1}$ at two different concentrations (0.2 and 0.4 μM). The reaction buffer contained E1 (UBA1), E2 (UbcH5b), FLAG-tagged ubiquitin (Ub), and NusA-Vpr-ΔC. Ubiquitinated proteins were detected by immunoblotting with either anti-UNG2 or anti-FLAG antibody after separation of the reaction mixture on SDS−PAGE and transfer to nitrocellulose.

mutations, 1LL/EE and 2LL/EE, were introduced into a Trx-peptide fusion construct, and fusion proteins and the DCAF1 809−876 peptide were purified to homogeneity (Figure 3C). The quaternary states of Trx-DCAF1 809−876, Trx-DCAF1 809−876 1LL/EE, and Trx-DCAF1 809−876 2LL/EE were analyzed by a multiangle light scattering. The experimental molecular mass of Trx-DCAF1 809−876 was derived as 51 kDa, significantly higher than the monomeric theoretical molecular mass (27 kDa) by almost 2-fold (Figure 3D, ▼). The estimated molecular masses of the Trx-DCAF1 1LL/EE and 2LL/EE proteins were 33 and 28 kDa, respectively, close to the theoretical monomer molecular masses (Figure 3D, ◆ and ●, respectively). For comparison, the unfused Trx protein eluted as a monomer (experimental and theoretical molecular mass of ~18 kDa, ■). These light scattering data strongly suggest that indeed the LisH motif of DCAF1 is responsible for oligomerization, with the Leu repeat providing critical determinants at the interface. To monitor potential structural changes in the LisH motif upon Leu residue mutation, the Trx-DCAF1 809−876 WT, 1LL/EE, and 2LL/EE fusion proteins were cleaved with TEV protease and DCAF1 peptides purified (Figure 4A, insert). The circular dichroism (CD) spectrum of the cleaved DCAF1 809−876 WT peptide exhibited two minima at 208 and 222 nm, indicating the presence of α-helical structure (Figure 4, circles). The monomeric DCAF1 LL/EE mutants, however, exhibited CD spectra characteristic of random coil structure (Figure 4, triangles and squares), suggesting that the four Leu repeat is essential for helix formation. For other LisH motif containing genes, it has been reported that disease-related mutations in this motif that abrogate oligomerization affect protein half-life and alter cellular localization (*54*, *55*). In the present case, WT DCAF1 and LL/EE mutants in transiently transfected HEK293 cells essentially exhibited the same half-life (data not shown).

The Adaptor−Receptor Complex, DDB1−DCAF1, Dimerizes via the DCAF1 Helical Domain. DDB1 is an adaptor protein that binds to the scaffolding protein complex, CUL4A-RBX1, and the substrate receptor, DCAF1, forming the E3 ubiquitin ligase. To evaluate the quaternary state of the adaptor−receptor complex, DDB1 complexes containing the 817−1507 DCAF1 constructs were purified and analyzed by light scattering (Figure 5). The observed molecular mass (411 kDa) of this complex is twice its theoretical value (DDB1, 130 kDa; DCAF1 817−1507, 81 kDa), lending further support to the finding that the region encompassing the LisH motif of DCAF1 mediates dimerization of the DDB1−DCAF1 complexes.

Electron Microscopy (EM) and 2D Image Analysis Suggest a Dimeric CRL^{DCAF1} Organization. For electron microscopy, we reconstituted the entire CRL4^{DCAF1} E3 ubiquitin ligase complex from its four components. As evidenced by SDS−PAGE (Figure 6A), the four individual proteins in the complex are present in equimolar amounts (CUL4A, 87 kDa; RBX1, 12 kDa; DDB1, 130 kDa; DCAF1 817−1507, 81 kDa) resulting in an overall molecular mass of the complex of 650 kDa by light scattering, confirming its dimeric quaternary state (Figure 6B). However, some smaller species, possibly subcomplexes, are also observed upon 50-fold dilution to 50 nM concentration (necessary for EM analysis). The larger particles represent the intact complex (Figure 6C). They are well separated from each other and appear to be homogeneous with similar sizes after uranyl acetate staining. From EM projection images, the estimated diameter of a sphere required for enclosing these large particles is about 180 Å, significantly larger than what would be expected for a monomeric, 310 kDa CRL4^{DCAF1} particle. Classification of approximately 1900 particle images by multivariant statistical analysis from the raw micrographs resulted in the class averages depicted in Figure 6D. Near-mirror symmetries were observed for a few of the 2D class averages (Figure 6D), suggesting the presence of a 2-fold axis in the particles. Therefore, the EM study of CRL4^{DCAF1} particles agrees well with the biochemical analyses described above.

Possible Roles of Dimerization of DCAF1 in Ubiquitin Ligase Activity of CRL4$^{DCAF1\text{-}Vpr}$. Dimerization of the CUL4A-RING E3 ligase can impart functional advantages onto the ligase complex, such as permitting productive loading of different size and shape substrates for ubiquitination. Many other ubiquitin E3 ligases dimerize via substrate receptor proteins. For example, in some Skp1-Cdc53/Cul1-F-box (SCF) E3 ligases, a small dimerization domain (D-box) is located within the substrate receptor protein (*56*, *57*). It is believed that dimerization of CRLs imparts variability in the overall geometry of the complexes, permitting ubiquitination of substrates *in cis* as well as *in trans* (*40*−*44*).

The ubiquitination activities of monomeric and dimeric CRL4^{DCAF1} E3 ligases were tested using DCAF1 817−1507 (dimeric) or DCAF1 1005−1507 (monomeric) constructs (Figure 7A). Although it is not clear which cellular substrates are targeted by CRL4^{DCAF1}, we previously demonstrated that uracil DNA glycosylase 2 (UNG2) becomes ubiquitinated via CRL4^{DCAF1} in a Vpr-dependent manner (*46*). Ubiquitin transfer activity of dimeric CRL4^{DCAF1} is more than 2-fold higher than that of a monomeric complex (Figure 7B, compare lanes 2−4 with 6−8 and lanes 10−12 with 14−16), supporting the notion that dimerization of substrate recognition proteins allows for more efficient ubiquitin transfer. However, other possible reasons for the observed difference could also be related to the missing region between the LisH motif and the start of the WD40 domain in monomeric CRL4^{DCAF1}.

Previous structural data of DDB1 have revealed that the relative orientation of CUL4A-binding domain is variable relative to the substrate receptor-binding domains, creating different distances between CUL4A-RBX1 and the substrate (*19*−*21*). This also may facilitate ubiquitination of substrates, and dimerization of DCAF1 potentially could add further conformational variability. However, it should be noted that the LisH motif is not commonly present among putative DCAF substrate receptors (*58*), and further structural and biochemical studies are necessary to fully evaluate the conformational variability in these complexes.

CONCLUSIONS

DCAF1, initially identified as a HIV-1 Vpr binding protein (VprBP) and belonging to the large family of WD40 domain containing substrate receptors of CUL4-RING E3 ubiquitin ligases, forms an adaptor−receptor complex with DDB1. Although several of DCAF1's biological functions have been described, our understanding of its activity in proteasomal degradation of target substrates still remains refractory. In this report, we demonstrate that a stretch of Leu residues in the LisH sequence motif is essential for oligomerization. The LisH motif is embedded in a region of ca. 40 amino acids (~840−880) that possesses helical structure and is located N-terminal to the WD40 domain of DCAF1. This region is important for dimerization of the CRL4 complex, and dimeric CRL4^{DCAF1} appears to possess enhanced Vpr-mediated ubiquitin transfer activity, compared to its mutant monomeric counterpart.

ACKNOWLEDGMENT

We thank Dr. Teresa Brosenitsch for critical reading of the manuscript and Thomas Vu and Mathieu Cuchanski for expert technical assistance. We also thank Dr. Jacek Skowronski for communication of unpublished results.

REFERENCES

1. Goldstein, G., Scheid, M., Hammerling, U., Schlesinger, D. H., Niall, H. D., and Boyse, E. A. (1975) Isolation of a polypeptide that has lymphocyte-differentiating properties and is probably represented universally in living cells. *Proc. Natl. Acad. Sci. U.S.A. 72*, 11–15.
2. Ciechanover, A., Finley, D., and Varshavsky, A. (1984) Ubiquitin dependence of selective protein degradation demonstrated in the mammalian cell cycle mutant ts85. *Cell 37*, 57–66.
3. Ciechanover, A., Finley, D., and Varshavsky, A. (1984) The ubiquitin-mediated proteolytic pathway and mechanisms of energy-dependent intracellular protein degradation. *J. Cell. Biochem. 24*, 27–53.
4. Hershko, A., and Ciechanover, A. (1998) The ubiquitin system. *Annu. Rev. Biochem. 67*, 425–479.
5. Pickart, C. M. (2001) Mechanisms underlying ubiquitination. *Annu. Rev. Biochem. 70*, 503–533.
6. Hicke, L. (2001) Protein regulation by monoubiquitin. *Nat. Rev. Mol. Cell. Biol. 2*, 195–201.
7. Hough, R., Pratt, G., and Rechsteiner, M. (1986) Ubiquitin-lysozyme conjugates. Identification and characterization of an ATP-dependent protease from rabbit reticulocyte lysates. *J. Biol. Chem. 261*, 2400–2408.
8. Pickart, C. M., and Fushman, D. (2004) Polyubiquitin chains: polymeric protein signals. *Curr. Opin. Chem. Biol. 8*, 610–616.
9. Liu, F., and Walters, K. J. (2010) Multitasking with ubiquitin through multivalent interactions. *Trends Biochem. Sci. 35*, 352–360.
10. Hershko, A., Heller, H., Elias, S., and Ciechanover, A. (1983) Components of ubiquitin-protein ligase system. Resolution, affinity purification, and role in protein breakdown. *J. Biol. Chem. 258*, 8206–8214.
11. Pickart, C. M., and Rose, I. A. (1985) Ubiquitin carboxyl-terminal hydrolase acts on ubiquitin carboxyl-terminal amides. *J. Biol. Chem. 260*, 7903–7910.
12. Pickart, C. M., and Rose, I. A. (1985) Functional heterogeneity of ubiquitin carrier proteins. *J. Biol. Chem. 260*, 1573–1581.
13. Petroski, M. D., and Deshaies, R. J. (2005) Function and regulation of cullin-RING ubiquitin ligases. *Nat. Rev. Mol. Cell. Biol. 6*, 9–20.
14. Kamura, T., Conrad, M. N., Yan, Q., Conaway, R. C., and Conaway, J. W. (1999) The Rbx1 subunit of SCF and VHL E3 ubiquitin ligase activates Rub1 modification of cullins Cdc53 and Cul2. *Genes Dev. 13*, 2928–2933.
15. Tan, P., Fuchs, S. Y., Chen, A., Wu, K., Gomez, C., Ronai, Z., and Pan, Z. Q. (1999) Recruitment of a ROC1-CUL1 ubiquitin ligase by Skp1 and HOS to catalyze the ubiquitination of I kappa B alpha. *Mol. Cell 3*, 527–533.
16. Wang, G., Yang, J., and Huibregtse, J. M. (1999) Functional domains of the Rsp5 ubiquitin-protein ligase. *Mol. Cell. Biol. 19*, 342–352.
17. Bosu, D. R., and Kipreos, E. T. (2008) Cullin-RING ubiquitin ligases: global regulation and activation cycles. *Cell Div. 3*, 7.

18. Merlet, J., Burger, J., Gomes, J. E., and Pintard, L. (2009) Regulation of cullin-RING E3 ubiquitin-ligases by neddylation and dimerization. *Cell. Mol. Life Sci. 66*, 1924–1938.
19. Li, T., Chen, X., Garbutt, K. C., Zhou, P., and Zheng, N. (2006) Structure of DDB1 in complex with a paramyxovirus V protein: viral hijack of a propeller cluster in ubiquitin ligase. *Cell 124*, 105–117.
20. Angers, S., Li, T., Yi, X., MacCoss, M. J., Moon, R. T., and Zheng, N. (2006) Molecular architecture and assembly of the DDB1-CUL4A ubiquitin ligase machinery. *Nature 443*, 590–593.
21. Scrima, A., Konickova, R., Czyzewski, B. K., Kawasaki, Y., Jeffrey, P. D., Groisman, R., Nakatani, Y., Iwai, S., Pavletich, N. P., and Thoma, N. H. (2008) Structural basis of UV DNA-damage recognition by the DDB1-DDB2 complex. *Cell 135*, 1213–1223.
22. Groisman, R., Polanowska, J., Kuraoka, I., Sawada, J., Saijo, M., Drapkin, R., Kisselev, A. F., Tanaka, K., and Nakatani, Y. (2003) The ubiquitin ligase activity in the DDB2 and CSA complexes is differentially regulated by the COP9 signalosome in response to DNA damage. *Cell 113*, 357–367.
23. Kapetanaki, M. G., Guerrero-Santoro, J., Bisi, D. C., Hsieh, C. L., Rapic-Otrin, V., and Levine, A. S. (2006) The DDB1-CUL4ADDB2 ubiquitin ligase is deficient in xeroderma pigmentosum group E and targets histone H2A at UV-damaged DNA sites. *Proc. Natl. Acad. Sci. U.S.A. 103*, 2588–2593.
24. He, Y. J., McCall, C. M., Hu, J., Zeng, Y., and Xiong, Y. (2006) DDB1 functions as a linker to recruit receptor WD40 proteins to CUL4-ROC1 ubiquitin ligases. *Genes Dev. 20*, 2949–2954.
25. Higa, L. A., Wu, M., Ye, T., Kobayashi, R., Sun, H., and Zhang, H. (2006) CUL4-DDB1 ubiquitin ligase interacts with multiple WD40-repeat proteins and regulates histone methylation. *Nat. Cell Biol. 8*, 1277–1283.
26. Jin, J., Arias, E. E., Chen, J., Harper, J. W., and Walter, J. C. (2006) A family of diverse Cul4-Ddb1-interacting proteins includes Cdt2, which is required for S phase destruction of the replication factor Cdt1. *Mol. Cell 23*, 709–721.
27. Higa, L. A., and Zhang, H. (2007) Stealing the spotlight: CUL4-DDB1 ubiquitin ligase docks WD40-repeat proteins to destroy. *Cell Div. 2*, 5.
28. Jackson, S., and Xiong, Y. (2009) CRL4s: the CUL4-RING E3 ubiquitin ligases. *Trends Biochem. Sci. 34*, 562–570.
29. Transy, C., and Margottin-Goguet, F. (2009) HIV1 Vpr arrests the cell cycle by recruiting DCAF1/VprBP, a receptor of the Cul4-DDB1 ubiquitin ligase. *Cell Cycle 8*, 2489–2490.
30. Le Rouzic, E., Morel, M., Ayinde, D., Belaidouni, N., Letienne, J., Transy, C., and Margottin-Goguet, F. (2008) Assembly with the Cul4A-DDB1DCAF1 ubiquitin ligase protects HIV-1 Vpr from proteasomal degradation. *J. Biol. Chem. 283*, 21686–21692.
31. Wen, X., Duus, K. M., Friedrich, T. D., and de Noronha, C. M. (2007) The HIV1 protein Vpr acts to promote G2 cell cycle arrest by engaging a DDB1 and Cullin4A-containing ubiquitin ligase complex using VprBP/DCAF1 as an adaptor. *J. Biol. Chem. 282*, 27046–27057.
32. Tan, L., Ehrlich, E., and Yu, X. F. (2007) DDB1 and Cul4A are required for human immunodeficiency virus type 1 Vpr-induced G2 arrest. *J. Virol. 81*, 10822–10830.
33. Le Rouzic, E., Belaidouni, N., Estrabaud, E., Morel, M., Rain, J. C., Transy, C., and Margottin-Goguet, F. (2007) HIV1 Vpr arrests the cell cycle by recruiting DCAF1/VprBP, a receptor of the Cul4-DDB1 ubiquitin ligase. *Cell Cycle* 182–188.
34. Hrecka, K., Gierszewska, M., Srivastava, S., Kozaczkiewicz, L., Swanson, S. K., Florens, L., Washburn, M. P., and Skowronski, J. (2007) Lentiviral Vpr usurps Cul4-DDB1[VprBP] E3 ubiquitin ligase to modulate cell cycle. *Proc. Natl. Acad. Sci. U.S.A. 104*, 11778–11783.
35. DeHart, J. L., Zimmerman, E. S., Ardon, O., Monteiro-Filho, C. M., Arganaraz, E. R., and Planelles, V. (2007) HIV-1 Vpr activates the G2 checkpoint through manipulation of the ubiquitin proteasome system. *Virol. J. 4*, 57.
36. Belzile, J. P., Duisit, G., Rougeau, N., Mercier, J., Finzi, A., and Cohen, E. A. (2007) HIV-1 Vpr-mediated G2 arrest involves the DDB1-CUL4AVPRBP E3 ubiquitin ligase. *PLoS Pathog. 3*, e85.
37. Belzile, J. P., Richard, J., Rougeau, N., Xiao, Y., and Cohen, E. A. (2010) HIV-1 Vpr induces the K48-linked polyubiquitination and proteasomal degradation of target cellular proteins to activate ATR and promote G2 arrest. *J. Virol. 84*, 3320–3330.
38. Saha, A., and Deshaies, R. J. (2008) Multimodal activation of the ubiquitin ligase SCF by Nedd8 conjugation. *Mol. Cell 32*, 21–31.
39. Duda, D. M., Borg, L. A., Scott, D. C., Hunt, H. W., Hammel, M., and Schulman, B. A. (2008) Structural insights into NEDD8 activation of cullin-RING ligases: conformational control of conjugation. *Cell 134*, 995–1006.
40. McMahon, M., Thomas, N., Itoh, K., Yamamoto, M., and Hayes, J. D. (2006) Dimerization of substrate adaptors can facilitate cullin-mediated ubiquitylation of proteins by a "tethering" mechanism: a two-site interaction model for the Nrf2-Keap1 complex. *J. Biol. Chem. 281*, 24756–24768.
41. Hao, B., Oehlmann, S., Sowa, M. E., Harper, J. W., and Pavletich, N. P. (2007) Structure of a Fbw7-Skp1-cyclin E complex: multisite-phosphorylated substrate recognition by SCF ubiquitin ligases. *Mol. Cell 26*, 131–143.
42. Welcker, M., and Clurman, B. E. (2007) Fbw7/hCDC4 dimerization regulates its substrate interactions. *Cell Div. 2*, 7.
43. Tang, X., Orlicky, S., Lin, Z., Willems, A., Neculai, D., Ceccarelli, D., Mercurio, F., Shilton, B. H., Sicheri, F., and Tyers, M. (2007) Suprafacial orientation of the SCFCdc4 dimer accommodates multiple geometries for substrate ubiquitination. *Cell 129*, 1165–1176.
44. Li, Y., and Hao, B. (2010) Structural basis of dimerization-dependent ubiquitination by the SCF(Fbx4) ubiquitin ligase. *J. Biol. Chem. 285*, 13896–13906.
45. Ahn, J., Byeon, I. J., Byeon, C. H., and Gronenborn, A. M. (2009) Insight into the structural basis of pro- and antiapoptotic p53 modulation by ASPP proteins. *J. Biol. Chem. 284*, 13812–13822.
46. Ahn, J., Vu, T., Novince, Z., Guerrero-Santoro, j., Rapic-Otrin, V., and Gronenborn, A. (2010) HIV-1 Vpr loads uracil DNA glycosylase-2 onto DCAF1, a substrate recognition subunit of a cullin 4A-RING E3 ubiquitin ligase for proteasome-dependent degradation. *J. Biol. Chem. 285*, 37333–37341.
47. Wishart, D. S., Bigam, C. G., Holm, A., Hodges, R. S., and Sykes, B. D. (1995) ^{1}H, ^{13}C and ^{15}N random coil NMR chemical shifts of the common amino acids. I. Investigations of nearest-neighbor effects. *J. Biomol. NMR 5*, 67–81.
48. Spera, S., Ikura, M., and Bax, A. (1991) Measurement of the exchange rates of rapidly exchanging amide protons: application to the study of calmodulin and its complex with a myosin light chain kinase fragment. *J. Biomol. NMR 1*, 155–165.
49. Ludtke, S. J., Baldwin, P. R., and Chiu, W. (1999) EMAN: semiautomated software for high-resolution single-particle reconstructions. *J. Struct. Biol. 128*, 82–97.
50. Chew, E. H., Poobalasingam, T., Hawkey, C. J., and Hagen, T. (2007) Characterization of cullin-based E3 ubiquitin ligases in intact mammalian cells--evidence for cullin dimerization. *Cell. Signal. 19*, 1071–1080.
51. Emes, R. D., and Ponting, C. P. (2001) A new sequence motif linking lissencephaly, Treacher Collins and oral-facial-digital type 1 syndromes, microtubule dynamics and cell migration. *Hum. Mol. Genet. 10*, 2813–2820.
52. Kim, M. H., Cooper, D. R., Oleksy, A., Devedjiev, Y., Derewenda, U., Reiner, O., Otlewski, J., and Derewenda, Z. S. (2004) The structure of the N-terminal domain of the product of the lissencephaly gene Lis1 and its functional implications. *Structure 12*, 987–998.
53. Mateja, A., Cierpicki, T., Paduch, M., Derewenda, Z. S., and Otlewski, J. (2006) The dimerization mechanism of LIS1 and its implication for proteins containing the LisH motif. *J. Mol. Biol. 357*, 621–631.
54. Gerlitz, G., Darhin, E., Giorgio, G., Franco, B., and Reiner, O. (2005) Novel functional features of the Lis-H domain: role in protein dimerization, half-life and cellular localization. *Cell Cycle 4*, 1632–1640.
55. Boulton, S. J., Brook, A., Staehling-Hampton, K., Heitzler, P., and Dyson, N. (2000) A role for Ebi in neuronal cell cycle control. *EMBO J. 19*, 5376–5386.
56. Wolf, D. A., McKeon, F., and Jackson, P. K. (1999) F-box/WD-repeat proteins pop1p and Sud1p/Pop2p form complexes that bind and direct the proteolysis of cdc18p. *Curr. Biol. 9*, 373–376.
57. Suzuki, H., Chiba, T., Suzuki, T., Fujita, T., Ikenoue, T., Omata, M., Furuichi, K., Shikama, H., and Tanaka, K. (2000) Homodimer of two F-box proteins betaTrCP1 or betaTrCP2 binds to IkappaBalpha for signal-dependent ubiquitination. *J. Biol. Chem. 275*, 2877–2884.
58. Lee, J., and Zhou, P. (2007) DCAFs, the missing link of the CUL4-DDB1 ubiquitin ligase. *Mol. Cell 26*, 775–780.